

Article

Improved Radar Detection of Small Drones Using Doppler Signal-to-Clutter Ratio (DSCR) Detector

Jiangkun Gong ¹ , Jun Yan ^{1,*}, Huiping Hu ², Deyong Kong ³ and Deren Li ¹

¹ State Key Laboratory of Information Engineering in Surveying, Mapping and Remote Sensing, Wuhan University, Wuhan 430072, China; gjk@whu.edu.cn (J.G.); drli@whu.edu.cn (D.L.)

² Wuhan Geomatics Institute, Wuhan 430022, China; huhuiping@whu.edu.cn

³ School of Information Engineering, Hubei University of Economics, Wuhan 430205, China; kdykong@hbue.edu.cn

* Correspondence: yanjun_pla@whu.edu.cn; Tel.: +86-027-68778527

Abstract: The detection of drones using radar presents challenges due to their small radar cross-section (RCS) values, slow velocities, and low altitudes. Traditional signal-to-noise ratio (SNR) detectors often fail to detect weak radar signals from small drones, resulting in high “Missed Target” rates due to the dependence of SNR values on RCS and detection range. To overcome this issue, we propose the use of a Doppler signal-to-clutter ratio (DSCR) detector that can extract both amplitude and Doppler information from drone signals. Theoretical calculations suggest that the DSCR of a target is less dependent on the detection range than the SNR. Experimental results using a Ku-band pulsed-Doppler surface surveillance radar and an X-band marine surveillance radar demonstrate that the DSCR detector can effectively extract radar signals from small drones, even when the signals are similar to clutter levels. Compared to the SNR detector, the DSCR detector reduces missed target rates by utilizing a lower detection threshold. Our tests include quad-rotor, fixed-wing, and hybrid vertical take-off and landing (VTOL) drones, with mean SNR values comparable to the surrounding clutter but with DSCR values above 10 dB, significantly higher than the clutter. The simplicity and low radar requirements of the DSCR detector make it a promising solution for drone detection in radar engineering applications.

Keywords: drone detection; Doppler signal-to-clutter ratio (DSCR); missed target; signal-to-noise ratio (SNR)



Citation: Gong, J.; Yan, J.; Hu, H.; Kong, D.; Li, D. Improved Radar Detection of Small Drones Using Doppler Signal-to-Clutter Ratio (DSCR) Detector. *Drones* **2023**, *7*, 316. <https://doi.org/10.3390/drones7050316>

Academic Editors: Bo Li, Chunwei Tian, Daqing Chen and Ming Yan

Received: 17 April 2023

Revised: 4 May 2023

Accepted: 8 May 2023

Published: 10 May 2023



Copyright: © 2023 by the authors. Licensee MDPI, Basel, Switzerland. This article is an open access article distributed under the terms and conditions of the Creative Commons Attribution (CC BY) license (<https://creativecommons.org/licenses/by/4.0/>).

1. Introduction

Detecting drones (or unmanned aerial vehicles, UAVs) using radar poses a significant challenge due to their slow velocities and small radar cross-section (RCS) values [1–6], which can result in a high number of missed targets. Common drone types include multirotor drones, helicopters, and unmanned fixed-wing aircraft [7–10]. Furthermore, the issue of drone swarms is expected to pose a significant challenge for the counter-drone industry in the future [11–14]. This vulnerability can lead to drones being used as ghost spies, silently invading borders and threatening coastal border defenders, highlighting the importance of developing counter-drone technologies.

Small drones are characterized by their small RCS, slow speeds, and low altitudes. These drones typically fall into Group 1 (Table 1) as reported by the U.S. Department of Defense, which requires rotating blades for aerial flight [10]. Group 1 drones generally have an RCS of 0.01–0.1 m², which is approximately 1/10,000 to 1/1000 the size of a typical airplane. Current radar detectors use the amplitude detection, Doppler detection, and other improved detectors, but traditional signal-to-noise ratio (SNR) detectors often result in a missed target due to weak radar signals from the small RCS values of drones [15]. Researchers have developed different methods to suppress background clutter and improve the SNR of targets, such as a constant false alarm rate (CFAR) and modified CFAR

detectors [16–19]. Additionally, Doppler detectors, including moving target detection (MTD) [20] and track-before-detection (TBD) technology, have been developed for detecting drones [21–24], although the latter requires a long tracking period and may struggle with sudden drone hovering.

Table 1. Drone classification according to the U.S. Department of Defense (DoD) ^{1,2}.

Category	Size	Maximum Gross Takeoff Weight (Pounds)	Normal Operating Altitude (ft)	Airspeed (Knots)
Group 1	Small	<20	<1200 AGL ³	<100
Group 2	Medium	21–55	<3500 AGL	<250
Group 3	Large	<1320	<18,000 MSL ⁴	<250
Group 4	Larger	>1320	<18,000 MSL	Any airspeed
Group 5	Largest	>1320	>18,000 MSL	Any airspeed

¹ Source: “Eyes of the Army”, U.S. Army Roadmap for UAS 2010–2035 [10]. <https://home.army.mil/rucker/index.php>, accessed on 4 May 2023; ² If the drone has even one characteristic of the next level, it is classified in that level. ³ AGL = Above Ground Level. ⁴ MSL = Mean Sea Level.

Due to the limitations of current detectors that rely on SNR values, which are affected by the small RCS values of drones, there is a need to develop a detector that is independent of RCS values. To address this issue, we propose a new detector that extracts the Doppler signal-to-clutter ratio (DSCR) of targets. The DSCR detector is capable of detecting radar signals in almost real time and does not require tracking. In this study, we present the algorithm for the DSCR detector in Section 2 and compare its performance with actual radar data in Section 3. We consider different detection ranges, background clutter, and drone types. The experimental results demonstrate that the DSCR detector outperforms the traditional SNR detector. In Section 4, we analyze the difference between missed targets and false alarms. Finally, we conclude our findings in Section 5.

2. Materials and Methods

2.1. Theoretical Model

The classical method of radar detection involves detecting signals in noise along the range dimension and using the SNR to determine the ratio between the target signal power and the mean noise level. Figure 1 shows three possible outcomes: “False Alarm”, “Detected Target”, and “Missed Target”. A “False Alarm” occurs when the detected signals are not from the target, while a “Missed Target” represents a situation where the signal power is below the detection threshold of the SNR detector. Although radar detection does not explicitly involve an identification process, it still incorporates it implicitly because it is necessary to distinguish between “False Alarm” and “Missed Target” (or “Missed Alarm”). In the case of small-slow targets, “Missed Alarm” is a common problem due to their low signal power, which can be similar to the mean noise level. Therefore, reducing “Missed Target” should be a priority when detecting small-slow targets to increase detection probability. Once the “Missed Target” are minimized, automatic target recognition (ATR) technology can be employed to classify between a “False Alarm” and a “Detected Target” to lower false alarms rate and maintain high detection probability.

The traditional radar detector assumes that a target is a point object with a mean RCS. This detector calculates the SNR, which is a measure of a radar’s ability to detect a specific target at a given range, by comparing the prioritized scattering power of a target over the background. The SNR is an essential parameter used to maintain the detection probability, which is calculated by [17]:

$$SNR \text{ (dB)} = 10 \log_{10} \left(\frac{E_r}{E_n} \right) = 10 \log_{10} \left(\frac{P_t G_r G_t \lambda^2 \sigma}{(4\pi)^3 R^4 K T_s B_n L} \right) \quad (1)$$

where E_r = the power of radar echoes from a target and E_n = the power of noise. T_s = the system noise temperature, B_n = the noise bandwidth of the receiver, L = the

total system losses, K = the Boltzmann's constant. P_t = the transmitted power, G_r = the received gain, G_t = the transmitted gain, R = the measured range, σ = the radar cross section (RCS) of the target, λ = the radar wavelength. For a certain radar, its transmitted parameters are given, and then Equation (1) can be revised into

$$SNR \propto \frac{\sigma}{R^4} \quad (2)$$

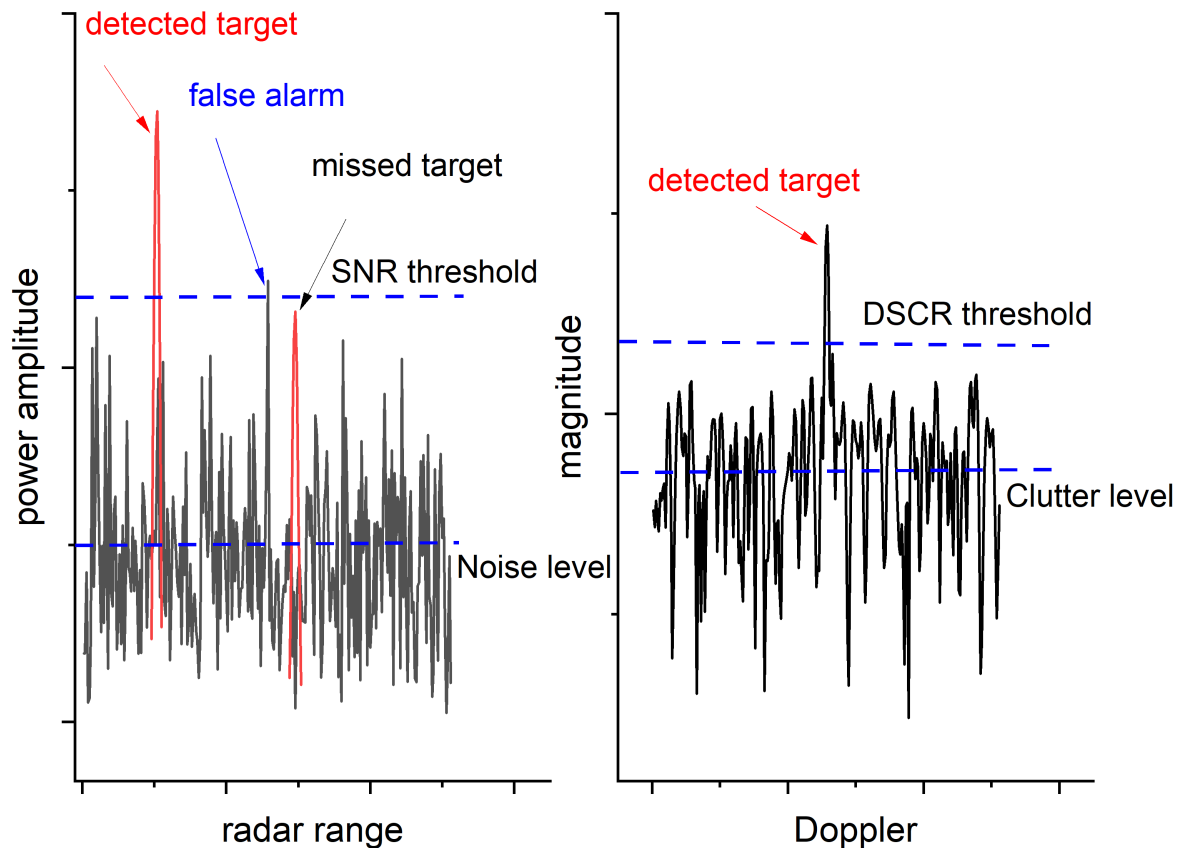


Figure 1. The detection of signals in noise and clutter (**Left:** SNR detector, **Right:** DSCR detector).

Equation (2) demonstrates that the SNR of a target is a function of its RCS and the detection range. The basic radar detector is the threshold detection, which can be represented as

$$P_{SNR} \geq SNR_{thr} \quad (3)$$

where SNR_{thr} = the threshold of the SNR detector, and P_{SNR} = the measured SNR value of the target. For single pulse detection, if the detection probability exceeds 50%, the target's SNR should be at least 13.1 dB, and to achieve a 95% probability, the SNR should be 16.8 dB [17]. In simpler terms, a smaller target with a lower RCS will have a lower SNR, resulting in a shorter detection range. Thus, radar systems often encounter the problem of "Missed Target" when detecting drones and other objects with small RCS values.

It is widely acknowledged that targets are not merely point objects, but rather distributed ones. This notion is supported by the observation of micro-Doppler phenomena, as described by micro-Doppler theory [25–27]. For instance, when it comes to a drone, its spectrum contains body Doppler, micro-Doppler, and clutter Doppler components. The body Doppler in the spectrum is induced by the Doppler effect, which is expressed as follows:

$$\overline{f_{bd}} = -\frac{2V_b}{\lambda} \quad (4)$$

where V_b = the flying speed of the target, λ = the radar wavelength. Secondly, micro-motion can be characterized as a simple periodic motion superimposed on the main movement of the target, and the micro-Doppler shifts in the spectrum is given by

$$\overline{f_{md}(t)} = \frac{L}{\lambda} \omega \cos \beta \cos(\omega t) + \overline{f_{bd}} \quad (5)$$

where L = the length of the micro-structure, β = the elevation angle, and ω = the rotating speed. Thus, the Doppler spectra of targets always contain generalized Doppler peaks, which include both micro-Doppler, body Doppler shifts and clutter shifts, as given by

$$\overline{f_d(t)} = \overline{f_{bd}} + \overline{f_{md}(t)} + \overline{f_{cd}(t)} \quad (6)$$

where $\overline{f_{bd}}$ = the body Doppler vector, $\overline{f_{md}(t)}$ = the body micro-Doppler vector, and $\overline{f_{cd}(t)}$ = the clutter Doppler vector, which are related to the clutter. Here, we use the term "generalized Doppler" to describe Doppler, including body Doppler and micro-Doppler.

We introduce a novel parameter to quantify the strength of the generalized Doppler signal in a radar spectrum. Specifically, given radar data $X(n)$ within a single radar resolution cell, and the corresponding Doppler spectrum $F(k)$, we define the Doppler signal-to-clutter ratio (DSCR) of a Doppler frequency D within this cell as follows:

$$DSCR(D)(dB) = 10 \log_{10} \left[\frac{F(D)}{\frac{\sum_{K=1}^N F(K)}{N}} \right] \quad (7)$$

where $F(K)$ = the amplitude of frequencies in the spectrum of the current radar bin; K = the Doppler frequency in the spectrum; and N = the length of the spectrum. D could be either the body Doppler or micro-Doppler, or even any Doppler in the spectrum. Radar echoes in one radar bin include the scattering power of the target and the background clutter, and the Doppler effect can extract the scattering part of the target (i.e., $F(D)$) from the background (i.e., $F(K)$). It should be noted that while Equation (4) only considers the body Doppler shift components in the spectrum, the DSCR in Equation (7) takes into account both the magnitude of the Doppler component and the Doppler speed. Compared to Equations (1) and (2), because the DSCR uses no value related to the RCS value of the target, it is independent of the detection range.

2.2. Algorithm Description

Here, we propose a concise detector using the above DSCR value for detecting radar signals of drones, which combines amplitude detection and Doppler detection, as shown in Algorithm 1. The steps for the DSCR detector are as follows:

- (1) Obtain the radar echoes raw data, $X(n)$, in one radar resolution cell, and calculate its Doppler spectrum, $F(K)$.
- (2) Search the spectrum, $F(K)$, to locate the strongest Doppler shift of D starting from the beginning point of M . Generally, we assume that the Doppler points below M belong to the background clutter. Calculate the maximum DSCR of the strongest Doppler shift of D .
- (3) Compare the value of the maximum DSCR with the detection threshold T . If the DSCR is above the threshold, then it is a target. Otherwise, it is not.

We believe that this method is effective for detecting drones and can provide near-real-time results without the need for a tracking period.

Before using the DSCR detector, two parameters are required: the spreading width of the background clutter (i.e., the beginning point of M) and the detection threshold (i.e., the detection threshold of T). These parameters are determined based on statistical data from the specific scenario. The spreading width of the background clutter (or the beginning point) depends on the type of clutter. For a ground clutter, a fixed length of M can be used, but for a sea clutter, an adaptive method to adjust the width of M is preferable due

to its time–space variance. The detection threshold of the DSCR detector can be either hard-style or soft-style. The hard threshold is based on the bottom noise level of the radar system and is typically set at twice the bottom noise level. For example, if the radar system has a bottom noise level of 5 dB, the DSCR detector threshold can be set at 8 dB. The soft threshold requires mean statistical data from the scenario and allows the DSCR detector to automatically adjust the threshold to adapt to new scenarios.

Algorithm 1: Calculating the maximum DSCR value.

```

1:   Function begins:
2:   Compute the Fourier transform of  $X(n)$  using fast Fourier transform (FFT), store it in  $F(k)$ .
3:   Initialize a variable  $Ma$  to zero.
4:   while each index  $i$  from  $M$  to  $N-M$ , do
5:     if  $F(i) > Ma$ , then
6:       update  $Ma$  to  $F(i)$  and  $D$  to  $i$ .
7:     end if
8:   end while
9:   Compute the mean value of  $F(k)$  and store it in a variable  $Me$ .
10:  Compute the spectral contrast ratio (DSCR),  $Ds$ , as the ratio of  $Ma$  to  $Me$ .
11:  Translate the  $Ds$  into a dB value using  $10\log_{10}(Ds)$ .
12:  Return the values of  $Ds$  and  $D$ .
13:  Function end.

```

2.3. Experimental Tests

In addition to the theoretical calculations, we use real radar data to verify the comparison between the SNR and DSCR values of drones.

(1) Ku-band radar test

We first conducted experiments to evaluate the performance of the DSCR detector using data collected by a Ku-band pulsed-Doppler phased array radar (surface surveillance radar) with a coherent pulse integration (CPI) of approximately 30 ms and a pulse repetition frequency (PRF) of 6 kHz. The radar has a range resolution of 15 m. The data were collected at the Yellow River wetland bird protection area in China, which includes various environments such as roads, rivers, farmlands, and woods with moving targets such as vehicles, people, flocks of sheep, and birds. We used a DJI Phantom 3 drone, manufactured by DJI Inc. (Shenzhen, China) in our experiment, which is a quadcopter with propellers in a tractor configuration. The drone's body and propellers are primarily composed of plastic, while the individual rotors are made of carbon fiber and plastic. The drone weighs 1.280 kg, has a maximum horizontal flight speed of 57.6 km/h, and a maximum rotor blade rotary speed of $150^\circ/\text{s}$. It can fly up to a maximum height of 6000 m and has a flight time of 23 min. It should be noted that the drone used in our experiment is not the same as the one shown in Figure 2.



Figure 2. The test environment using the Ku-band radar.

(2) X-band radar test

We also utilized a pulse-Doppler phased array radar (maritime surveillance radar) operating in the X-band, in addition to the Ku-band radar, to validate the DSCR detector. The radar had a PRF of approximately 5 kHz, a CPI of about 20 ms and a range resolution of 12 m. It had an active electronically scanned phased array antenna, and the raw data collected were float complex data. To evaluate the DSCR detector, we used three drones as cooperative targets, and their specifications are provided in Table 2, with their images displayed in Figure 3. We collected data from various coastal areas, including the cities of Qidong and Rizhao in China. Figure 3 indicates the relative positions of the drones with respect to the radar. During the tests, the Qidong sea had a lower sea scale than Class 3, while the Rizhao sea had a sea scale of approximately Class 5. To distinguish between the two sea scales, we referred to the former as the “Qidong sea” and the latter as the “Rizhao sea” in this study. However, these names are not indicated on any official maps. Additionally, we collected radar data in the ground clutter background in Nanjing city.

Table 2. Parameters of the drones.

Drone Type	Hybrid VTOL Fixed-Wing	Multirotor	Fixed-Wing
Model	TX25A	Phantom 4	Albatross 1
Manufacturer	Harryskydream Inc.	DJI Inc.	Homemade
Flight weight	26 kg	1.38 kg	0.3 kg
Wingspan	360 cm	40 cm	108 cm
Body size	197 cm	40 cm	80 cm
Blade length	30 cm	20 cm	10 cm
Rotor number	5	4	2
Cruise speed	25 m/s	15 m/s	10 m/s
Aero-frame materials	FRP (Fiber reinforced plastic)	PC (Polycarbonate)	EPP (Expanded polypropylene)

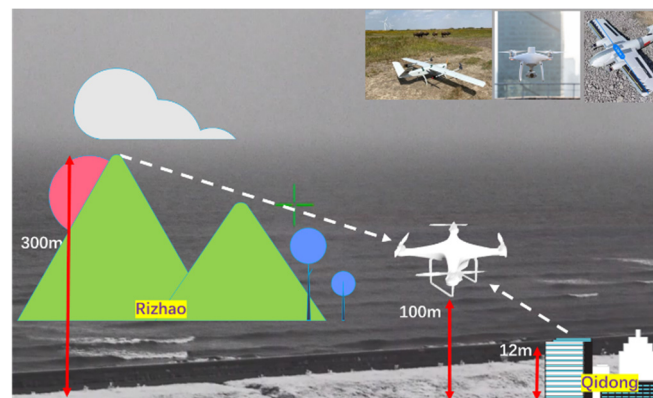


Figure 3. The relative locations between the drones and the radar in the tests using the X-band radar.

3. Results

3.1. Simulated Result

We conducted simulations to demonstrate the DSCR of radar signals from a drone. Figure 4a shows the simulated raw data of radar signals from a drone where $x(n)$ is the time series and $f(k)$ is the spectrum. $x(n)$ is given by:

$$x(n) = 8e^{2\pi \times 0.5n \times j} + 4e^{2\pi \times 20n \times j} + 2e^{2\pi \times 40n \times j} + 3 \times \text{randn}(\text{size}(n)) \quad (8)$$

where n = the sample data from 1 to 256; $\text{size}(n)$ = the MATLAB function calculating the size of a variable. $\text{randn}(n)$ = the MATLAB function providing the normally distributed pseudorandom numbers. The sampling frequency is 256. Figure 4a shows three digital frequencies of 0.5, 20, and 40, with magnitudes of 5.06, 3.84, and 1.94, respectively. We assume the clutter Doppler to be $0.5 + \text{randn}$ and the body Doppler of the drone to be 20,

while the micro-Doppler of the drone produced by the blade is 40. Many sources contribute to the clutter, such as environmental and biological clutter (e.g., birds) when the radar detects drones. Thereby, clutters could have low Dopplers (e.g., environmental clutter) around 0 and high Dopplers (e.g., biological clutter) such as 78 in Figure 4b.

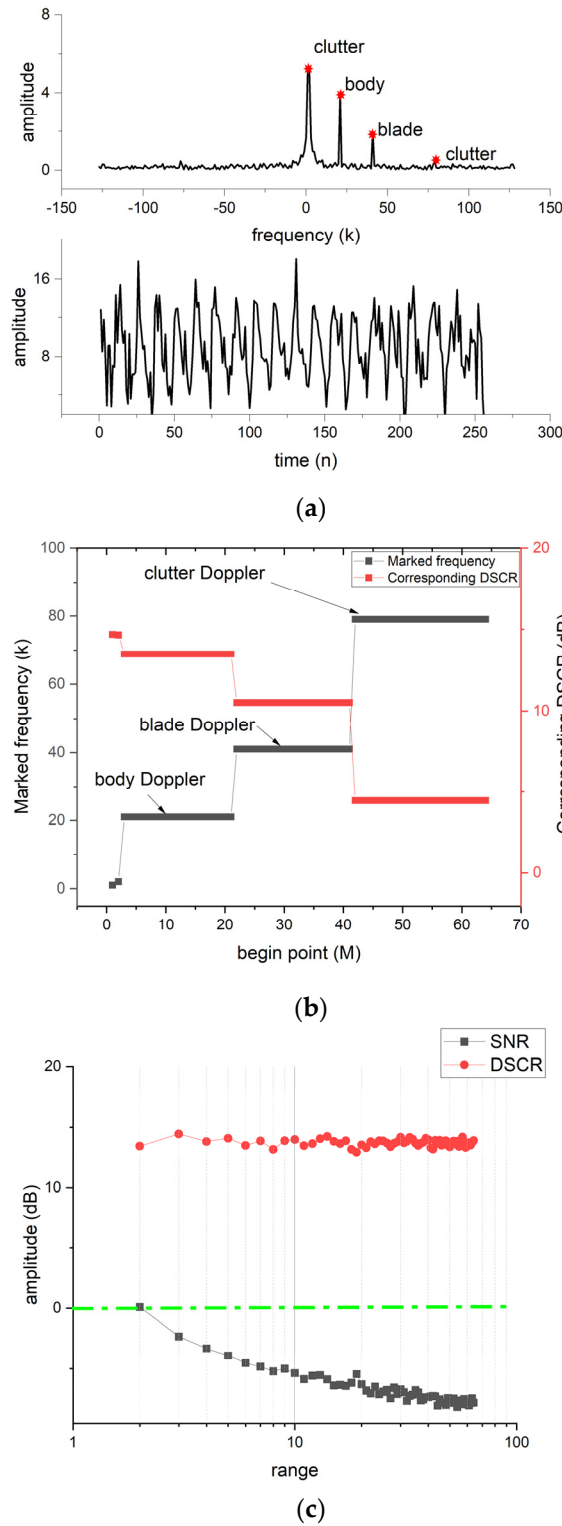


Figure 4. Simulated radar data to calculate the DSCR of signals: (a) raw signals and their spectrum, (b) the relationship between the beginning point from 1 to 64 and the DSCR value, as well as the marked digital frequency, (c) comparison of SNR and DSCR values given different range factors.

The DSCR of a Doppler is closely related to the choice of the beginning point of M in Step (2). Figure 4b illustrates the impact of varying the beginning point of M on the calculated DSCR values. As M is changed from 1 to 64, the marked Doppler frequency D and the corresponding DSCR value also change. In most cases, the body Doppler of 20 and the blade Doppler of 40 are correctly identified as D , and their corresponding DSCR values exhibit only slight fluctuations. Therefore, it is important to select M carefully to accurately identify the body Doppler of 20. If M is either too small or too large, the marked body Doppler frequency will be incorrect.

The impact of the detection range on the DSCR of radar signals is minimal compared to that of the SNR. Figure 4c compares the SNR and DSCR of radar signals under different detection ranges. The radar signals affected by the detection range are represented as follows:

$$y(n) = A \times x(n) \quad (9)$$

where A = the transmission loss of radar signals related to the range [28]. With the noise threshold level set as 64, M as 8, and D as 20, Figure 4c illustrates the decay in amplitude of $y(n)$ with an increasing detection range. The values are dimensionless. The green dotted line denotes the detection threshold of 0 dB, and as the detection range factor increases, the SNR values of the signals also decrease from 0.08 dB to -8.09 dB. In contrast, the DSCR values remain relatively stable, fluctuating between 14.46 dB and 12.97 dB. The standard deviation of DSCR is only 0.28, which accounts for just 19% of the 1.46 SNR value. Equation (7) shows that the denominator of the DSCR is the mean value of the entire spectrum; therefore, the DSCR is largely unaffected by the detection range.

3.2. Real Ku-Band Radar Data

The DSCR detector effectively separates the radar signals of the drone from the background clutter in the frequency spectrum. Figure 5 displays the normalized data and Doppler spectra of both the drone and the clutter. MATLAB's signal processing tools, specifically the FFT function, were utilized to obtain the spectra from the raw time data. The drone's spectrum reveals a dominant bulk Doppler, corresponding to the drone's body Doppler, with a maximum DSCR value of 17.24 dB and a speed of -2.7 m/s indicating that the drone was flying away from the radar. Conversely, there is no bulk Doppler evident in the clutter spectrum, with the Doppler magnitudes being uniform, suggesting the absence of objects in the clutter radar data.

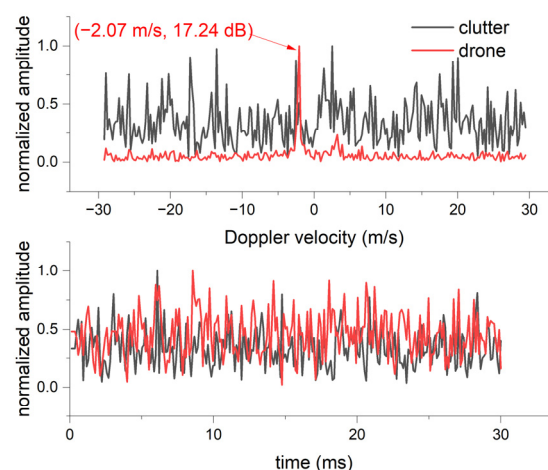


Figure 5. Ku-band raw radar data and Doppler spectra of a quad-rotor drone and clutter in one radar cell.

The results of the tracking demonstrate the ability of the DSCR detector to detect weak radar signals of the drone in a clutter. The tracking results of the SNR, DSCR, and Doppler speeds of the drone are presented in Figure 6. In most cases, the SNR of the drone

is similar to that of the clutter within the same range. The tracking range is approximately 1.3 km from the radar location, with a mean SNR of the drone of about 0.93 dB, similar to the clutter's 0.003 dB. The dynamic range of the drone's clutter is 3.45 dB, larger than the clutter's 2.41 dB, indicating that the RCS of the drone changes with radar observation angles and the drone's radar signals are weak, similar to the clutter level. Therefore, traditional SNR detectors may have difficulty in detecting radar echoes from the drone.

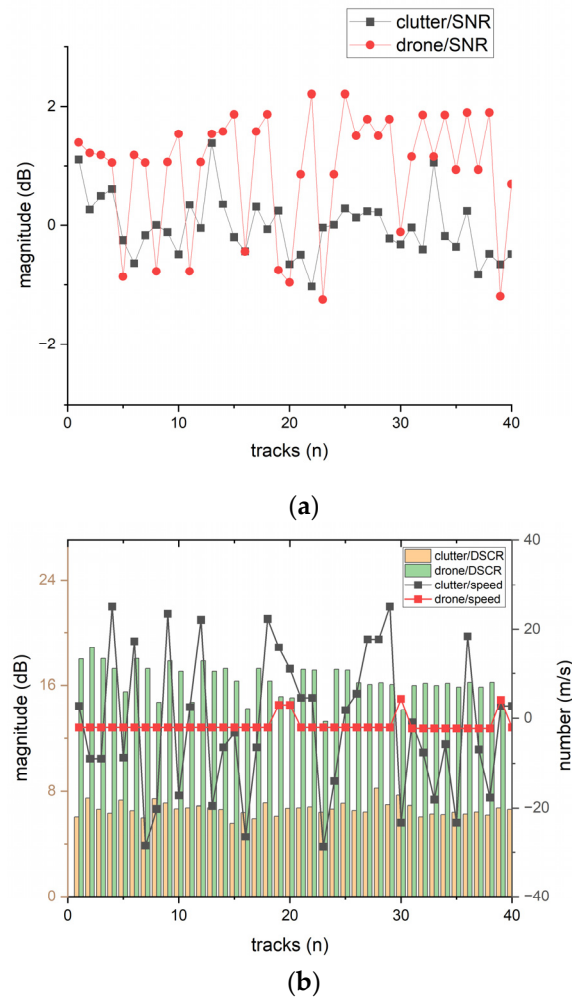


Figure 6. Ku-band tracking SNR and DSCR values of a quad-rotor drone, (a) SNR comparison of the clutter and the drone, (b) DSCR comparison of the clutter and the drone.

However, the DSCR detector can detect such weak radar signals from the drone. In most cases, the DSCR of the drone is much larger than that of the clutter in Figure 6b. The mean DSCR of the drone is approximately 16.28 dB, about 10 dB larger than the clutter's 6.67 dB, and approximately 13 dB larger than the SNR of the drone. This suggests that the detection threshold can be lowered by at least 10 dB. According to the radar Equation (1), a 10 dB improvement means that the radar distance of the same target will be enhanced by approximately 77% when given the false alarm probability and detection probability. Alternatively, a different target with a much smaller RCS value of 90% can be detected. Therefore, the DSCR detector is superior to the SNR detector in detecting radar signals from the drone because it has a lower detection threshold. Furthermore, Figure 6b shows that the DSCR detector also extracts the body Doppler speeds of the drone. The dynamic range of the drone's Doppler is only 2.3 m/s, much smaller than the clutter's 27.83 m/s, with a standard deviation of 0.50 m/s, much smaller than the clutter's 8.57 m/s. The body Dopplers of the drone have a pattern, whereas the Dopplers of the clutter appear random.

3.3. Real X-Band Radar Data

The DSCR detector analyzes the spectrum of radar signals over time to detect targets. Figure 7 shows the raw X-band data and Doppler spectra of drones. The raw data's amplitude is normalized and dimensionless. We processed the raw time data using signal processing tools, including the FFT function in MATLAB, to obtain the spectrum. We collected radar data from hybrid vertical take-off and landing (VTOL) and quad-rotor drones in a sea clutter background and from a fixed-wing drone in a ground clutter background. The quad-rotor drone, hybrid VTOL drone, and fixed-wing drone have max DSCR values of 9.41 dB, 9.91 dB, and 13.18 dB, respectively, with Doppler velocities of -6.9 m/s, -15.6 m/s, and 8.7 m/s. A negative Doppler indicates flying away from the radar. Sea clutter or ground clutter can cause a spreading Doppler, which may suppress a drone's body Doppler if it is flying at a low speed.

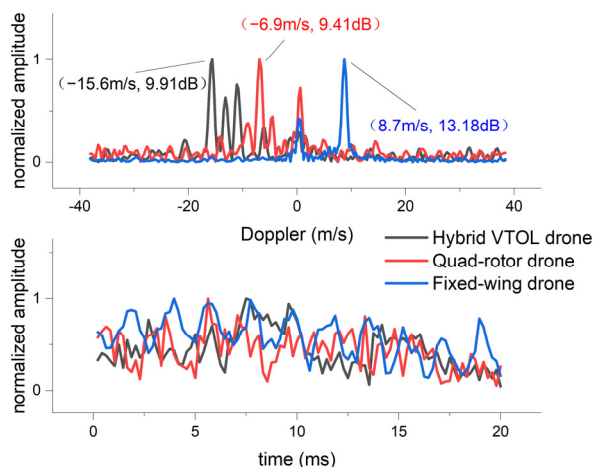


Figure 7. X-band raw radar data and Doppler spectra of drones in one radar cell.

The DSCR detector outperforms the SNR detector in detecting targets. In Figure 8, we present the detection results of a quad-rotor drone in a range window comprising 20 radar bins. This area has a length of 240 m since the range resolution is 12 m. The drone was located in radar bin #12. The DSCR values denote the maximum DSCR in each radar cell, whereas the SNR values are true numbers. In the Qidong case, the quad-rotor drone was about 10 km away from the radar, and the range was roughly 5.7 km in the Rizhao case. The SNR of the drone was almost zero in the Qidong data. However, the SNR value was higher (approximately 6 dB) when the detection range was shorter. Additionally, the elevation angle beams and different sea classes are also considered, as shown in Figure 3.

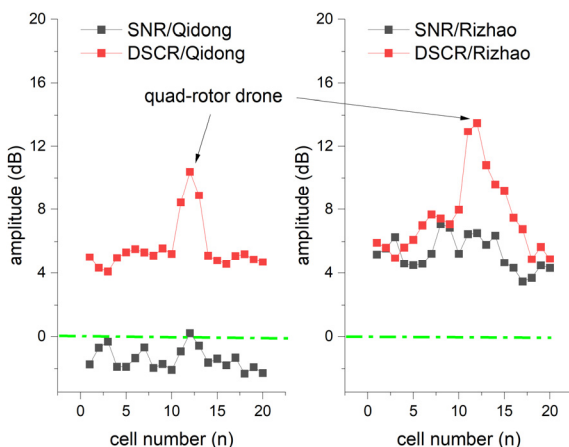


Figure 8. The SNR and DSCR values of the 20 radar bins detected at ranges of 10 km in the Qidong case and 5 km in the Rizhao case, where the drone is in radar cell #12.

The clutter in the Rizhao case has higher SNR values than that in the Qidong case. Three reasons may explain this difference. Firstly, the SNR values represent the received power when using the same radar system, and they are not the SNR values when using a CFAR detector. Secondly, the data in the Rizhao case were detected at approximately half of the detection range of that in the Qidong case, and the SNR of targets and clutter could be larger in the Qidong case based on the radar equation. Thirdly, the data in the Rizhao case were detected with a look-down angle, and the clutter mainly came from the sea clutter. On the other hand, the data in the Qidong case were detected with a look-up angle, and the clutter data were generated by the air. Therefore, the SNR values in the Rizhao case were much higher than those in the Qidong case.

However, the SNR values of the drone are comparable to the surrounding clutter SNR values in each case. The SNR values of both the air clutter and the drone in the Qidong case were around 0 dB, while those of both the sea clutter and the drone were approximately 6 dB in the Rizhao case. Sometimes, the SNR of the drone was smaller than that of the surrounding clutter. For instance, the SNR in radar bin #6 in the Rizhao case was higher than that of the drone in radar bin #12. Therefore, the SNR detector failed to detect the drone in both cases. In contrast, the DSCR values of the drone (i.e., 10.3 dB and 13.5 dB) were more stable in the two cases, and the DSCR detector successfully detected the drone in both cases.

4. Discussion

A “Missed Target” occurs when the signal power of the target is lower than the SNR detector’s detection threshold, while a “False Alarm” indicates that the detected signals are not from the target. Although the identification process is not explicitly stated in radar detection, it is necessary to classify a missed target and false alarm. “Missed Targets” are the most common situations in detecting drones because they have small RCS values resulting in low signal power, similar to the RMS noise level. Therefore, reducing missed targets to zero should be a priority in drone detection.

The DSCR detector has the advantage of having a lower missed target rate but the disadvantage of a high false alarm rate, without the ability to differentiate between the clutter and the target. To reduce the false alarm rate, automatic target recognition (ATR) technology can be used after detection by the DSCR detector. The Swerling-I model suggests that a target’s SNR should be at least 13.1 dB to achieve a detection probability of over 50% and 16.8 dB for a probability of 95%. However, in most cases of detecting radar signals from drones, the SNR values of drones are significantly lower than the required values. Table 3 shows the statistical results of radar detection, where “MIN” and “MAX” represent the minimum and maximum values, respectively. “MEAN” is the mean value, while “STDEV” represents the standard deviation. Additionally, “STDEV/MEAN” is the ratio between the standard deviation and the mean value. The mean SNR values of drones are lower than the corresponding DSCR values, with a difference of 8.55, 10.05, and 11.43 for the VTOL drone, quad-rotor drone, and fixed-wing drone, respectively. This suggests that the DSCR detector can detect signals with a lower threshold than the SNR detector, or reduce the missed target rate compared to the SNR detector when using the same threshold. Furthermore, the “STDEV/MEAN” of the three drones’ SNR is almost 50%, whereas that of the DSCR is only 10%, as shown in Figure 9. It is important to note that these numbers were measured at a fixed range, and if different ranges were considered, the “STDEV/MEAN” values of the SNR could be worse as the SNR is dependent on the detection range. Overall, in addition to the DSCR values of a drone being higher than the SNR, the DSCR is also much more stable than the SNR.

The DSCR detector offers two distinct advantages over the SNR. Firstly, it extracts relative values that demonstrate relativity both in space and time. By utilizing radar data within one range unit across different distance bins, the DSCR detector effectively limits the scattering energy of the background clutter while preserving the scattering power of the target, resulting in an increased detection probability. Additionally, the short

radar dwell time of one range bin during one CPI significantly reduces interference from the background clutter and removes much of the time-varying background clutter. This relativity results in DSCR values that are almost independent of the detection range, and the detector combines the advantages of amplitude detection and Doppler detection. By transforming radar signals from the time domain into the frequency domain using Fourier transformation, the Doppler frequency contains both the amplitude and velocity of the target, providing a powerful tool for detection.

Table 3. Performance of different detection methods.

Drone Types		Hybrid VTOL Drone	Quad-Rotor Drone	Fixed-Wing Drone
Detection Background		Sea	Sea	Ground
Detection Ranges		8~14 km	10 km	5 km
SNR	MIN (dB)	2.58	0.20	0.70
	MAX (dB)	8.07	4.28	5.13
	MEAN (dB)	4.83	1.76	2.59
	STDEV (dB)	1.86	1.18	1.19
	STDEV/MEAN	0.38	0.67	0.46
DSCR	MIN (dB)	11.24	10.06	11.09
	MAX (dB)	17.08	14.13	16.83
	MEAN (dB)	13.38	11.81	14.02
	STDEV (dB)	1.38	1.15	1.52
	STDEV/MEAN	0.10	0.09	0.11

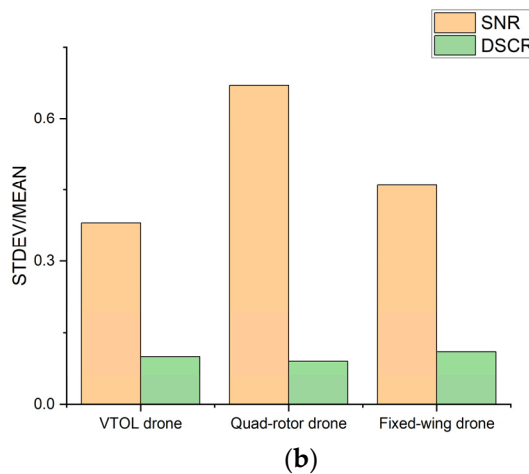
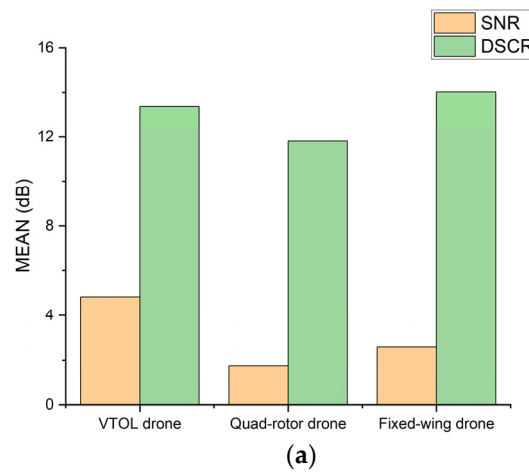


Figure 9. The comparison of SNR and DSCR values of the three drones: (a) the mean values, (b) the ratio between the standard deviation and the mean value.

Secondly, Fourier transformation enables the classification of different scattering sources into distinct spectral parts. While the clutter tends to concentrate in the low-frequency part, targets fall into other parts of the spectrum. Even the body Doppler of drones due to their slow speed can fall into the clutter part, but the micro-Doppler due to the rotating blades can jump out of the clutter. The DSCR detector can effectively extract radar signals from targets such as drones, making it a useful and versatile tool in engineering applications.

In addition to the basic DSCR detector described in Section 2, the DSCR value can be utilized in other improved solutions for radar detection and classification. Table 4 provides a comparison of different solutions for detecting drones, highlighting the importance of designing effective detection and recognition algorithms to minimize both missed targets and false alarms. A combined approach using the DSCR detector and automatic target recognition (ATR) technology can effectively address the radar challenge of countering drones by reducing missed targets and false alarms. Therefore, reducing missed targets in drone detection is crucial, and the DSCR detector, together with ATR technology, can offer an effective solution.

Table 4. Different solutions for detecting drones.

Solutions	Detection	Recognition
Solution 1	SNR detector	Kinetic features (e.g., trace)
Solution 2	SNR detector	Signals signatures (e.g., micro-Doppler)
Solution 3	DSCR detector	Kinetic features (e.g., trace)
Solution 4	DSCR detector	Signals signatures (e.g., micro-Doppler)

5. Conclusions

The primary challenge in radar surveillance of drones is the high rate of “Missed Targets” due to their small RCS values, which limit the effectiveness of traditional SNR detectors. In this study, we propose a comparative method based on the DSCR value, which combines the advantages of amplitude and Doppler detection. Our results with Ku-band and X-band radars indicate that the SNR detector is ineffective in detecting drones due to cases of almost 0 dB-level SNR values. Although the DSCR detector may increase the number of false alarms, it can effectively reduce missed targets. However, an effective ATR solution is required to reduce false alarms. The DSCR detector is a detection tool, and effective ATR technology can recognize the objects detected by the DSCR detector and reduce false alarms. In our future work, we plan to investigate Solutions 3 and 4 in Table 4. Additionally, we will research adaptive methods using the DSCR detector.

Author Contributions: Conceptualization, J.Y.; methodology, J.G.; software, J.G.; validation, J.Y.; formal analysis, J.G.; investigation, J.Y.; resources, D.L.; data curation, J.Y.; writing—original draft preparation, J.G.; writing—review and editing, H.H.; visualization, H.H.; supervision, J.Y.; project administration, D.L.; funding acquisition, D.K. All authors have read and agreed to the published version of the manuscript.

Funding: This research received some support from the Natural Science Foundation of Hubei Providence (General Program: 2021CFB309).

Institutional Review Board Statement: Not applicable.

Informed Consent Statement: Not applicable.

Data Availability Statement: Some of the data presented in this study may be available on request from the corresponding author. The data are not publicly available due to the internal restriction of the research group.

Acknowledgments: We appreciate both the testers during the collection of the data, and we also want to thank the authors whose photographs are reproduced in this study.

Conflicts of Interest: The authors declare that they have no conflict of interest.

References

1. Čisar, P.; Pinter, R.; Čisar, S.M.; Gligorijević, M. Principles of Anti-Drone Defense. In Proceedings of the 2020 11th IEEE International Conference on Cognitive Infocommunications (CogInfoCom), Online on MaxWhere 3D Web, 23–25 September 2020; pp. 19–26.
2. Shi, X.; Yang, C.; Xie, W.; Liang, C.; Shi, Z.; Chen, J. Anti-Drone System with Multiple Surveillance Technologies: Architecture, Implementation, and Challenges. *IEEE Commun. Mag.* **2018**, *56*, 68–74. [\[CrossRef\]](#)
3. Gong, J.; Yan, J.; Li, D.; Kong, D.; Hu, H. Interference of Radar Detection of Drones By Birds. *Prog. Electromagn. Res. M* **2019**, *81*, 1–11. [\[CrossRef\]](#)
4. Markow, J.; Balleri, A.; Catherall, A. Statistical analysis of in-flight drone signatures. *IET Radar Sonar Navig.* **2022**, *16*, 1737–1751. [\[CrossRef\]](#)
5. Svanström, F.; Alonso-Fernandez, F.; Englund, C. Drone Detection and Tracking in Real-Time by Fusion of Different Sensing Modalities. *Drones* **2022**, *6*, 317. [\[CrossRef\]](#)
6. Ezuma, M.; Anjinappa, C.K.; Funderburk, M.; Guvenc, I. Radar Cross Section Based Statistical Recognition of UAVs at Microwave Frequencies. *IEEE Trans. Aerosp. Electron. Syst.* **2022**, *58*, 27–46. [\[CrossRef\]](#)
7. HECHT, E. Drones in the Nagorno-Karabakh War: Analyzing the Data. Available online: <https://www.militarystrategymagazine.com> (accessed on 3 May 2023).
8. Park, S.; Kim, H.T.; Lee, S.; Joo, H.; Kim, H. Survey on Anti-Drone Systems: Components, Designs, and Challenges. *IEEE Access* **2021**, *9*, 42635–42659. [\[CrossRef\]](#)
9. Wellig, P.; Speirs, P.; Schuepbach, C.; Oechsli, R.; Renker, M.; Boeniger, U.; Pratisto, H. Radar systems and challenges for C-UAV. In Proceedings of the International Radar Symposium, Bonn, Germany, 20–22 June 2018; pp. 1–8.
10. U.S. Army UAS Center of exCellenCe. “Eyes of the Army” U.S. Army Roadmap for Unmanned Aircraft Systems 2010–2035; U.S. Army: Arlington County, VA, USA, 2010.
11. Zheng, J.; Chen, R.; Yang, T.; Liu, X.; Liu, H.; Su, T.; Wan, L. An Efficient Strategy for Accurate Detection and Localization of UAV Swarms. *IEEE Internet Things J.* **2021**, *8*, 15372–15381. [\[CrossRef\]](#)
12. Zheng, J.; Yang, T.; Liu, H.; Su, T.; Wan, L. Accurate Detection and Localization of Unmanned Aerial Vehicle Swarms-Enabled Mobile Edge Computing System. *IEEE Trans. Ind. Inform.* **2021**, *17*, 5059–5067. [\[CrossRef\]](#)
13. Qi, D.; Zhang, J.; Liang, X.; Li, Z.; Zuo, J.; Lei, P. Autonomous Reconnaissance and Attack Test of UAV Swarm Based on Mosaic Warfare Thought. In Proceedings of the 2021 6th International Conference on Robotics and Automation Engineering (ICRAE), Guangzhou, China, 19–22 November 2021; pp. 79–83.
14. Zhou, Y.; Rao, B.; Wang, W. UAV Swarm Intelligence: Recent Advances and Future Trends. *IEEE Access* **2020**, *8*, 183856–183878. [\[CrossRef\]](#)
15. Dale, H.; Baker, C.; Antoniou, M.; Jahangir, M.; Atkinson, G.; Harman, S. SNR-dependent drone classification using convolutional neural networks. *IET Radar Sonar Navig.* **2022**, *16*, 22–33. [\[CrossRef\]](#)
16. VizcarroCarretero, M.; Harmanny, R.I.A.; Trommel, R.P. Smart-CFAR, a machine learning approach to floating level detection in radar. In Proceedings of the EuRAD 2019—2019 16th European Radar Conference, Paris, France, 2–4 October 2019; pp. 161–164.
17. Skolnik, M.I. *Introduction to Radar Systems*; McGraw Hill Book Co.: New York, NY, USA, 1999; Volume 19.
18. Humphreys, E.; Antoniou, M.; Baker, C.; Stafford, W. Cognitive Approaches to Detection of Small Targets. In Proceedings of the EuRAD 2020—2020 17th European Radar Conference, Utrecht, The Netherlands, 10–15 January 2021; pp. 366–369.
19. Roldan, I.; del-Blanco, C.R.; Duque de Quevedo, Á.; Ibañez Urzaiz, F.; Gismero Menoyo, J.; Asensio López, A.; Berjón, D.; Jaureguizar, F.; García, N. DopplerNet: A convolutional neural network for recognising targets in real scenarios using a persistent range-Doppler radar. *IET Radar Sonar Navig.* **2020**, *14*, 593–600. [\[CrossRef\]](#)
20. Tait, P. *Introduction to Radar Target Recognition*; Institution of Electrical Engineers: London, UK, 2006; ISBN 9781849190831.
21. Amrouche, N.; Khenchaf, A.; Berkani, D. Multiple target tracking using track before detect algorithm. In Proceedings of the 2017 19th International Conference on Electromagnetics in Advanced Applications, ICEAA 2017, Verona, Italy, 11–15 September 2017; pp. 692–695.
22. Buzzi, S.; Lops, M.; Venturino, L. Track-before-detect procedures for early detection of moving target from airborne radars. *IEEE Trans. Aerosp. Electron. Syst.* **2005**, *41*, 937–954. [\[CrossRef\]](#)
23. Kim, K.; Uney, M.; Mulgrew, B. Estimation of Drone Micro-Doppler Signatures via Track-Before-Detect in Array Radars. In Proceedings of the 2019 International Radar Conference (RADAR), Toulon, France, 23–27 September 2019. [\[CrossRef\]](#)
24. Guerraou, Z.; Khenchaf, A.; Comblet, F.; Leouffre, M.; Lacrouts, O. Particle Filter Track-Before-Detect for Target Detection and Tracking from Marine Radar Data. In Proceedings of the 2019 IEEE Conference on Antenna Measurements & Applications (CAMA), Kuta, Indonesia, 23–25 October 2019; pp. 1–4.
25. Chen, V.C. *The Micro-Doppler Effect in Radar*; Artech House: Norwood, MA, USA, 2011; ISBN 9781608070572.
26. Palamà, R.; Fioranelli, F.; Ritchie, M.; Inggs, M.; Lewis, S.; Griffiths, H. Measurements and discrimination of drones and birds with a multi-frequency multistatic radar system. *IET Radar Sonar Navig.* **2021**, *15*, 841–852. [\[CrossRef\]](#)

-
27. Hanif, A.; Muaz, M.; Hasan, A.; Adeel, M. Micro-Doppler Based Target Recognition With Radars: A Review. *IEEE Sens. J.* **2022**, *22*, 2948–2961. [[CrossRef](#)]
 28. Skolnik, M. *Radar Handbook*, 3rd ed.; McGraw-Hill Education: New York, NY, USA, 2008.

Disclaimer/Publisher’s Note: The statements, opinions and data contained in all publications are solely those of the individual author(s) and contributor(s) and not of MDPI and/or the editor(s). MDPI and/or the editor(s) disclaim responsibility for any injury to people or property resulting from any ideas, methods, instructions or products referred to in the content.